HHS Public Access

Author manuscript

Science. Author manuscript; available in PMC 2015 December 26.

Published in final edited form as:

Science. 2015 June 26; 348(6242): 1488–1492. doi:10.1126/science.aab3021.

Discrete Functions of Nuclear Receptor Rev-erbα Couple Metabolism to the Clock

Yuxiang Zhang[1,*], **Bin Fang**[1,*], **Matthew J. Emmett**[1], **Manashree Damle**[1], **Zheng Sun**[1,2], **Dan Feng**[1], **Sean M. Armour**[1], **Jarrett R. Remsberg**[1], **Jennifer Jager**[1], **Raymond E. Soccio**[1], **David J. Steger**[1], and **Mitchell A. Lazar**[1,†]

[1]Division of Endocrinology, Diabetes, and Metabolism, Department of Medicine, Department of Genetics, and the Institute for Diabetes, Obesity, and Metabolism, Perelman School of Medicine at the University of Pennsylvania, Philadelphia, PA 19104, USA

[2]Department of Molecular and Cellular Biology, Division of Diabetes, Endocrinology and Metabolism, Department of Medicine, Baylor College of Medicine, Houston, TX 77030, USA

SUMMARY

Circadian and metabolic physiology are intricately intertwined, as illustrated by Rev-erbα, a transcription factor (TF) that functions both as a core repressive component of the cell autonomous clock and as a regulator of metabolic genes. Here we show that Rev-erbα modulates the clock and metabolism by different genomic mechanisms. Clock control requires Rev-erbα to bind directly to the genome at its cognate sites, where it competes with activating ROR TFs. By contrast, Rev-erbα regulates metabolic genes primarily by recruiting the HDAC3 corepressor to sites to which it is tethered by cell type-specific transcription factors. Thus, direct competition between Rev-erbα and ROR TFs provides a universal mechanism for self-sustained control of molecular clock across all tissues, whereas Rev-erbα utilizes lineage-determining factors to convey a tissue-specific epigenomic rhythm that regulates metabolism tailored to the specific need of that tissue.

Circadian rhythmicity is a common feature of nearly all physiological processes (*1-4*). Each cell of the body contains a molecular clock comprised of transcription factors that act on one another in interlocking feedback loops that generate near-24 hour oscillations (*3, 5*). A core component of the molecular clock, the nuclear receptor Rev-erbα, is expressed with a circadian rhythm (*6*) and represses BMAL1, a positive regulator of clock output genes (*7*). Rev-erbα represses many genes, often to regulate metabolism in a circadian and tissue-dependent manner (*8-11*). Thus, Rev-erbα is central to complex interactions between the core clock and metabolism.

Since Rev-erbα is a core clock component but also has tissue-specific functions, we were interested in comparing its cistromes in different mouse tissues including liver, brain, and epididymal adipose tissue. The majority of Rev-erbα binding sites were tissue-specific (Fig. 1A), and gene ontology analyses were consistent with specialized functions of Rev-erbα

[†]To whom correspondence should be addressed. lazar@mail.med.upenn.edu.
[*]These authors contributed equally and should be considered first-authors

(fig. S1). However, a common Rev-erbα cistrome included binding at clock genes in all tissues, consistent with its universal function in the core clock (fig. S1) (*6*, *7*, *12*).

RevDR2 and RORE were the most enriched motifs at Rev-erbα binding sites shared among tissues (Fig. 1A), consistent with earlier reports that the function of Rev-erbα as a repressive component of the molecular clock involves binding to two RORE motifs that function in the transcriptional regulation of the *Bmal1* gene (*7*, *13*). Rev-erbα recruits the NCoR-HDAC3 complex to actively repress *Bmal1* transcription (*13*), and liver specific deletion of HDAC3 induced *Bmal1* expression (fig. S2B) at ZT10, consistent with previous reports *(9, 13)*. However, the loss of HDAC3 did not dampen circadian rhythmicity of *Bmal1* nor other clock components as much as the loss of Rev-erbα itself, suggesting an additional mechanism (figs. S2A-B).

Another, non-mutually exclusive mechanism posits competition with the activating nuclear receptor ROR for the DNA binding site, which contains RevDR2/RORE motifs bound by both receptors (*14-17*). The α and γ isoforms of ROR are most abundant in liver (*18*), and are expressed in a circadian manner with a peak at ZT18, antiphase to Rev-erbα (*19*), although the circadian variation of RORα is modest and of unclear biological significance (figs. S3A-B) (*19*). Liver specific deletion of RORα and γ markedly dampened the circadian oscillation of core clock genes in liver (figs. S3C-E), consistent with previous reports (*19*). To determine target genes common to RORs and Rev-erbα, we compared gene expressions in livers depleted of RORα and γ, at their peak time of expression, with gene expression from Rev-erbα knockout livers (*9*) (Fig. 1B). Intriguingly, genes regulated both by Rev-erbα and the RORs included clock genes such as *Bmal1*, *Npas2*, *Cry1*, and *E4bp4* (Fig. 1B, fig. S3F), and were expressed with large circadian amplitudes, consistent with the model that Rev-erbα and RORs are both critical regulators of the clock (Fig. 1C). By contrast, Rev-erbα-specific genes had modest circadian rhythms and were enriched for liver metabolic processes (Fig. 1C, fig. S3F).

Although RORα expression was similar at ZT10 and ZT22, there was a marked difference between RORα binding to ROREs at the clock genes *Bmal1* and *Npas2* at these times (fig. S4A). Deletion of Rev-erbα enhanced RORα recruitment to these sites at ZT10, and this was potentiated by loss of Rev-erbβ (Fig. 1D), consistent with lower binding of RORα at ZT10 being due to competition with Rev-erbs. Conversely, hepatic overexpression of Rev-erbα reduced RORα recruitment to *Bmal1* and *Npas2* sites at ZT22 (Fig. 1E). Genome-wide, ~44% of RORα binding sites overlapped with Rev-erbα, and these were more likely to be circadian than RORα-specific sites (Fig. 1F). In addition, sites of increased RORα binding at ZT22 were enriched for the RevDR2/RORE motifs bound by both Rev-erbα and RORα (figs. S4B-C). Moreover, oscillating RORα binding sites were enriched near common target genes of RORs and Rev-erbα (Fig. 1G), further suggesting that RORα and Rev-erbα compete for binding at highly circadian genes including core components of the molecular clock. In contrast, consistent with its expression, RORγ had a circadian binding pattern at overlapped and non-overlapped sites (fig. S4D).

To understand why Rev-erbα and ROR tended to compete near clock genes but not Rev-erbα-specific genes, we performed ChIP-exonuclease followed by high-throughput

sequencing (ChIP-exo) (*20*) in mouse liver at ZT10 to better resolve Rev-erbα binding (fig. S5A). At clock genes that regulated by Rev-erbα and RORs, exemplified by *Bmal1* and *Cry1*, the RevDR2/RORE motif was detected at ChIP-exo peaks (Fig. 2A, left). However, Rev-erbα ChIP-exo peaks were most commonly enriched for the motif bound by liver-lineage determining TF hepatocyte nuclear factor 6 (HNF6) (Fig. 2B). As exemplified by *Cyp2b13* and *Slc45a3*, these Rev-erbα binding sites co-localized with HNF6 in mouse liver (Fig. 2A, right). Overall, the HNF6 motif was found at 1,108 Rev-erbα ChIP-exo sites (Fig. 2C), the vast majority of which were also detected by HNF6 ChIP-exo in liver (*21*) yet did not have an RORE motif nearby (fig. S5B). The genes located nearest to these Rev-erbα/HNF6 binding sites ("Rev-erbα/HNF6-exo sites") were enriched for lipid metabolic processes (fig. S5C), similar to Rev-erbα-specific gene regulation. Indeed, enhancer RNAs (eRNAs) at these sites bound by Rev-erbα and HNF6 had a robust circadian expression pattern (Fig. 2D), and were markedly upregulated in livers depleted of Rev-erbα, indicating active repression of enhancer function at these sites (Fig. 2E) (*22*).

To test whether the binding of Rev-erbα on the genome can be indirect, we utilized a mouse model with a conditional deletion of the Rev-erbα DNA-binding domain (DBD). These mice have been previously studied as a model of Rev-erbα deletion (*12*, *23*), but the targeting strategy is predicted to lead to in-frame deletion of the DBD (fig. S6A) and Rev-erbα immunoblot of mouse liver after Cre-recombination revealed an abundant species at the approximate molecular weight of the protein lacking the DBD (fig. S6B). The identity of this protein as full-length Rev-erbα lacking its DBD was confirmed by mass spectrometric analysis of Rev-erbα immunoprecipitates from recombined liver extracts (fig. S6C). Thus, this model is actually a knock-in of a DBD mutation, rather than a complete knockout of the Rev-erbα protein. We studied the function of this Rev-erbα DBD mutant in mice whose livers were also depleted of Rev-erbβ to eliminate its compensatory effects (*6*, *12*).

ChIP-seq analysis of Rev-erbα in livers expressing only the Rev-erbα DBD mutant ("DBD^m") revealed a comparable level of binding at a subset of wild type sites ("DBD-independent sites"), while binding was dramatically reduced at many other sites ("DBD-dependent sites") (Fig. 2E, figs. S7A-B). HNF6 ChIP-seq signals (*24*) were more enriched at Rev-erbα DBD-independent sites than at the DBD-dependent sites (fig. S7C), suggesting that HNF6 might tether Rev-erbα to the DNA even in the absence of Rev-erbα DBD domain.

DBD-dependent sites were enriched in RORE as well as dimeric RevDR2 motifs, in agreement with direct DNA binding (fig. S7D). These motifs are also recognized by ROR, and indeed the binding of RORα at these sites decreased markedly at ZT10 when Rev-erbα competition is strongest (fig. S7E). RevDR2 were depleted in DBD-independent sites while ROREs still exist in a minority of sites (fig. S7D), suggesting RORE may facilitate, although not required for, DBD-independent binding. The HNF6 motif was markedly enriched at DBD-independent sites (fig. S7D), and Rev-erbα binding at Rev-erbα/HNF6-exo sites was comparable between wild type and DBD^m mice, following the same pattern as DBD-independent sites (fig. S7F). The simultaneous binding of Rev-erbα and HNF6 at these sites was confirmed by ChIP-re-ChIP experiments in wild type liver, whereas HNF6 and Rev-erbα were not co-localized at DBD-dependent sites (Fig. 2G, fig. S7G). Enhancer RNA

transcription showed circadian oscillation in phase ZT22, at DBD-dependent and -independent sites (fig. S7H), suggesting active repression of Rev-erbα in both cases. In agreement with Rev-erbα functioning by recruiting the corepressor complex, HDAC3 binding at Rev-erbα sites was reduced in Rev-erb-depleted livers (fig. S7I). In addition, the HDAC3 ChIP-seq signal in the DBD^{m} was reduced at DBD-dependent sites but not at sites that are DBD-independent (Fig. 2H), suggesting active repression by Rev-erbα via recruitment of HDAC3.

To determine whether HNF6 is required for Rev-erbα DBD-independent binding, we performed ChIP-seq for Rev-erbα in liver of 129S1/SvlmJ mice, and compared this result with that obtained in the C57BL/6J mice. The two strains differ by ~5.4 million single nucleotide polymorphisms (SNPs), and SNPs were predicted to cripple the HNF6 motif at 107 sites in C57BL/6J mice and 71 sites in 129S1/SvlmJ mice. Remarkably, Rev-erbα binding was markedly diminished at the sites in which the SNPs disrupt either RevDR2/RORE or HNF6 motif in C57BL/6J or 129S1/SvlmJ mice, while Rev-erbα binding at random SNPs tended to be unaffected (Figs. 3A-B, fig. S8A). Specific examples of strain-dependent binding of Rev-erbα at HNF6 sites are shown in Figs. 3A-B, and differential binding in the two mouse strains was confirmed by ChIP-PCR for HNF6 and Rev-erbα (figs. S8B-C). Interestingly, while the HNF6 motif was most significantly associated with strain specific Rev-erbα binding by the same analysis, we also found significant association with motifs for several other TFs that play important roles in liver function, suggesting involvement of other partners in Rev-erbα binding in the absence of RORE and RevDR2 (Fig. 3C).

The preserved binding of HDAC3, mediated by Rev-erbα DBD mutant, at metabolic genes suggested that hepatic expression of these genes might also be intact relative to livers of mice in which the Rev-erbα protein is deleted. To test this, we compared the gene expression changes in mice lacking Rev-erbα in liver with published results using the DBD^{m} mouse model used here, in which Rev-erbα is converted to the DBD mutant and Rev-erbβ is also deleted (*12*). Circadian clock genes were derepressed in both situations, demonstrating that that regulation of these genes required direct binding at RevDR2/RORE sites by Rev-erbα. Overall only ~25% of Rev-erbα target genes that were de-repressed in Rev-erbα KO mice were also de-repressed in the DBD^{m} mice (“DBD-dependent Rev-erbα targets”) (Fig. 4A). Genes de-repressed specifically in Rev-erbα KO mice (“DBD-independent Rev-erbα targets”) showed circadian expression peaking at ZT22 (fig. S9A), and were enriched for lipid metabolic functions (fig. S9B), suggesting that Rev-erbα regulates circadian lipid metabolic genes independent of its DBD. In support of this, DBD-independent Rev-erbα/HDAC3 sites were enriched near DBD-independent Rev-erbα targets, whereas DBD-dependent Rev-erbα/HDAC3 sites, where Rev-erbα and HDAC3 binding markedly reduced in DBD^{m} mice, were more enriched near DBD-dependent Rev-erbα targets (Fig. 4A). Examples of the deletion-specific regulation of metabolic genes are shown in Figs. 4B-C. Consistent with preserved metabolic gene expression in the DBD^{m} mice livers, these mice did not display hepatosteatosis as is characteristic of the mice with complete deletion of Rev-erbα (Figs. 4D-E, fig. S9C) (*6*, *9*).

These findings demonstrate that Rev-erbα has a DBD-independent function that contributes to its regulation of liver metabolism. Other nuclear receptors, including estrogen receptor and glucocorticoid receptor, have DBD-independent activities through protein-protein interactions with other TFs, either directly or indirectly (*25*, *26*). In liver, Rev-erbα is tethered to chromatin by hepatic lineage determining TFs (fig. S10), and this mechanism of binding explains much of the non-overlapping cistromes of Rev-erbα in different tissues as well as the large proportion of binding sites without the RevDR2/RORE motif. In liver, the tethered cistrome is more enriched for genes with specialized function in hepatic metabolism, whereas the DBD-dependent cistrome is enriched for circadian clock genes and common to multiple tissues.

Circadian clocks and metabolism are tightly connected (*1*, *3*, *4*), and Rev-erbα has emerged as a transcriptional link from circadian rhythms to metabolism in multiple tissues (*8*). Our findings delineate a molecular hierarchy that governs how the clock is wired with metabolism. Direct competition between Rev-erb and ROR provides a universal mechanism for self-sustained control of molecular clock across all tissues. On top of this basic landscape, circadianly expressed Rev-erb utilizes lineage-determination factors to convey a tissue-specific epigenomic rhythm that, through corepressor and HDAC3, regulates metabolism tailored to the specific need of that tissue. These two modes of action may bestow on Rev-erbα the ability to stabilize the circadian oscillations of clock gene, while coupling liver metabolism to environmental and metabolic changes, perhaps through its endogenous ligand heme (*27*, *28*). This raises the possibility that synthetic ligands which specifically affect Rev-erbα interaction with NCoR/HDAC3 without disrupting DNA-binding could modulate liver metabolism with lesser effects on the integrity of the circadian clock.

Supplementary Material

Refer to Web version on PubMed Central for supplementary material.

ACKNOWLEDGEMENTS

ChIP-seq and microarray data have been deposited in the Gene Expression Omnibus (GSE67973). We thank Simone Sidoli and Benjamin A. Garcia for assistance with mass spectrometry. We acknowledge the Functional Genomics Core and the Viral Vector Core of the Penn Diabetes Research Center (P30 DK19525) for next generation sequencing and virus preparation, respectively. We thank the Penn Digestives Disease Center Morphology Core (P30 DK050306) for histology studies and the Molecular Profiling Core for microarray analysis. This work was supported by NIH R01 DK45586 (MAL), K08 DK094968 (RES), R00 DK099443 (ZS), R01 DK098542 (DJS), F32 DK102284 (SMA), F30 DK104513 (MJE), T32 GM0008275 (JRR), and the Cox Medical Research Institute.

References

1. Feng D, Lazar MA. Clocks, metabolism, and the epigenome. Mol. Cell. 2012; 47:158–167. [PubMed: 22841001]
2. Asher G, Sassone-Corsi P. Time for food: The intimate interplay between nutrition, metabolism, and the circadian clock. Cell. 2015; 161:84–92. [PubMed: 25815987]
3. Takahashi JS, Hong HK, Ko CH, McDearmon EL. The genetics of mammalian circadian order and disorder: Implications for physiology and disease. Nat. Rev. Genet. 2008; 9:764–775. [PubMed: 18802415]

4. Bass J, Takahashi JS. Circadian integration of metabolism and energetics. Science. 2010; 330:1349–1354. [PubMed: 21127246]
5. Hardin PE, Panda S. Circadian timekeeping and output mechanisms in animals. Curr. Opin. Neurobiol. 2013; 23:724–731. [PubMed: 23731779]
6. Bugge A, et al. Rev-erbα and Rev-erbβ coordinately protect the circadian clock and normal metabolic function. Genes Dev. 2012; 26:657–667. [PubMed: 22474260]
7. Preitner N, et al. The orphan nuclear receptor Rev-erbα controls circadian transcription within the positive limb of the mammalian circadian oscillator. Cell. 2002; 110:251–260. [PubMed: 12150932]
8. Everett LJ, Lazar MA. Nuclear receptor Rev-erbα: Up, down, and all around. Trends Endocrinol. Metab. 2014; 25:586–592. [PubMed: 25066191]
9. Feng D, et al. A circadian rhythm orchestrated by histone deacetylase 3 controls hepatic lipid metabolism. Science. 2011; 331:1315–1319. [PubMed: 21393543]
10. Gerhart-Hines Z, et al. The nuclear receptor Rev-erbα controls circadian thermogenic plasticity. Nature. 2013; 503:410–413. [PubMed: 24162845]
11. Woldt E, et al. Rev-erb-α modulates skeletal muscle oxidative capacity by regulating mitochondrial biogenesis and autophagy. Nat. Med. 2013; 19:1039–1046. [PubMed: 23852339]
12. Cho H, et al. Regulation of circadian behaviour and metabolism by Rev-erb-α and Rev-erb-β. Nature. 2012; 485:123–127. [PubMed: 22460952]
13. Yin L, Lazar MA. The orphan nuclear receptor Rev-erbα recruits the N-CoR/histone deacetylase 3 corepressor to regulate the circadian Bmal1 gene. Mol. Endocrinol. 2005; 19:1452–1459. [PubMed: 15761026]
14. Giguere V, et al. Isoform-specific amino-terminal domains dictate DNA-binding properties of ROR alpha, a novel family of orphan hormone nuclear receptors. Genes Dev. 1994; 8:538–553. [PubMed: 7926749]
15. Forman BM, et al. Cross-talk among ROR alpha 1 and the Rev-erb family of orphan nuclear receptors. Mol. Endocrinol. 1994; 8:1253–1261. [PubMed: 7838158]
16. Harding HP, Lazar MA. The monomer-binding orphan receptor Rev-erb represses transcription as a dimer on a novel direct repeat. Mol. Cell. Biol. 1995; 15:4791–4802. [PubMed: 7651396]
17. Stashi E, et al. SRC-2 is an essential coactivator for orchestrating metabolism and circadian rhythm. Cell Rep. 2014; 6:633–645. [PubMed: 24529706]
18. Solt LA, Burris TP. Action of RORs and their ligands in (patho)physiology. Trends Endocrinol. Metab. 2012; 23:619–627. [PubMed: 22789990]
19. Takeda Y, Jothi R, Birault V, Jetten AM. RORgamma directly regulates the circadian expression of clock genes and downstream targets in vivo. Nucleic Acids Res. 2012; 40:8519–8535. [PubMed: 22753030]
20. Rhee HS, Pugh BF. Comprehensive genome-wide protein-DNA interactions detected at single-nucleotide resolution. Cell. 2011; 147:1408–1419. [PubMed: 22153082]
21. Wang L, et al. Mace: Model based analysis of ChIP-exo. Nucleic Acids Res. 2014; 42:e156. [PubMed: 25249628]
22. Fang B, et al. Circadian enhancers coordinate multiple phases of rhythmic gene transcription in vivo. Cell. 2014; 159:1140–1152. [PubMed: 25416951]
23. Lam MT, et al. Rev-erbs repress macrophage gene expression by inhibiting enhancer-directed transcription. Nature. 2013; 498:511–515. [PubMed: 23728303]
24. Faure AJ, et al. Cohesin regulates tissue-specific expression by stabilizing highly occupied cis-regulatory modules. Genome Res. 2012; 22:2163–2175. [PubMed: 22780989]
25. Heldring N, et al. Multiple sequence-specific DNA-binding proteins mediate estrogen receptor signaling through a tethering pathway. Mol. Endocrinol. 2011; 25:564–574. [PubMed: 21330404]
26. Glass CK, Saijo K. Nuclear receptor transrepression pathways that regulate inflammation in macrophages and T cells. Nat. Rev. Immunol. 2010; 10:365–376. [PubMed: 20414208]
27. Yin L, et al. Rev-erbα, a heme sensor that coordinates metabolic and circadian pathways. Science. 2007; 318:1786–1789. [PubMed: 18006707]
28. Raghuram S, et al. Identification of heme as the ligand for the orphan nuclear receptors Rev-erbα and Rev-erbβ. Nat. Struct. Mol. Biol. 2007; 14:1207–1213. [PubMed: 18037887]

29. Materials and methods are available as supplementary materials on science online

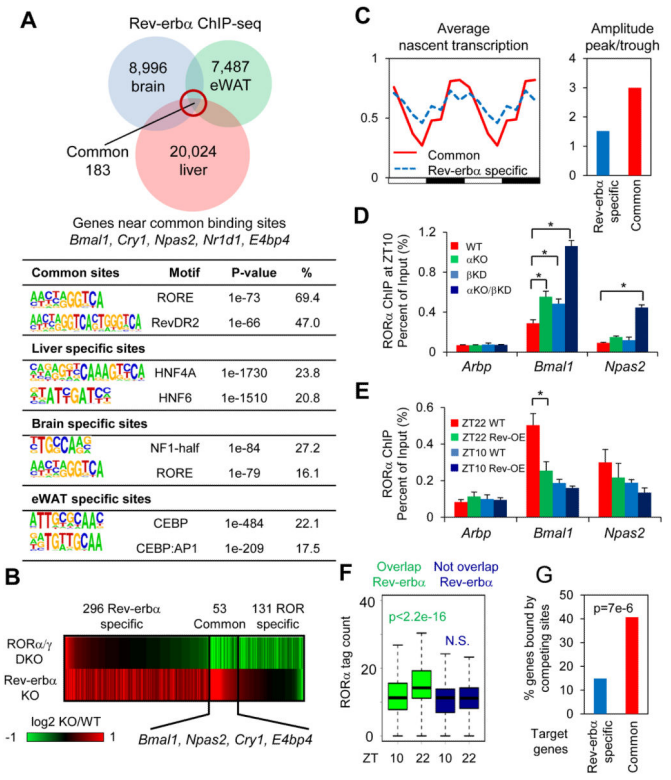

Figure 1. Rev-erbα represses clock genes by competing with RORα at its cognate sites

(A) Overlap of Rev-erbα cistromes in liver (*9*), brain and epididymal adipose tissue (eWAT). Most significantly enriched known motifs (abundance>10%) in common and tissue specific cistromes are shown. (B) Heat map showing expression fold changes of genes deactivated by RORα/γ double KO (DKO/WT< −1.3, p<0.01) and derepressed by Rev-erbα KO (αKO/WT>1.3, p<0.01). (C) Mean relative GRO-seq transcription (left) throughout 24-hour light dark cycle, as well as oscillation amplitudes (right) of RORs/Rev-erbα common targets (red) and Rev-erbα specific targets (blue). Time points were duplicated for clearer visualization. (D) RORα binding at clock and control genes promoters at ZT10, in wild type (WT), Rev-erbα KO (αKO), Rev-erbβ knockdown (βKD), and αKO/βKD mice liver, interrogated by ChIP-PCR. Data are expressed as mean± SEM (* Student's t-test, p<0.05, n=4). (E) RORα binding at clock and control genes promoters at ZT10 or ZT22 in Rev-erbα overexpression (OE) mouse liver, interrogated by ChIP-PCR. Data are expressed as mean± SEM (* Student's t-test, p<0.05, n=6 or 7). (F) Circadian binding of RORα at sites overlapped or not overlapped with Rev-erbα cistrome (N.S. Student's t-test, p>0.05). (G) Percentage of common or Rev-erbα specific target genes containing high confidence oscillating RORα binding sites (ZT22>2 reads per million (rpm), ZT22/ZT10>1.5) within 50kb of TSSs (P value from hypergeometric test).

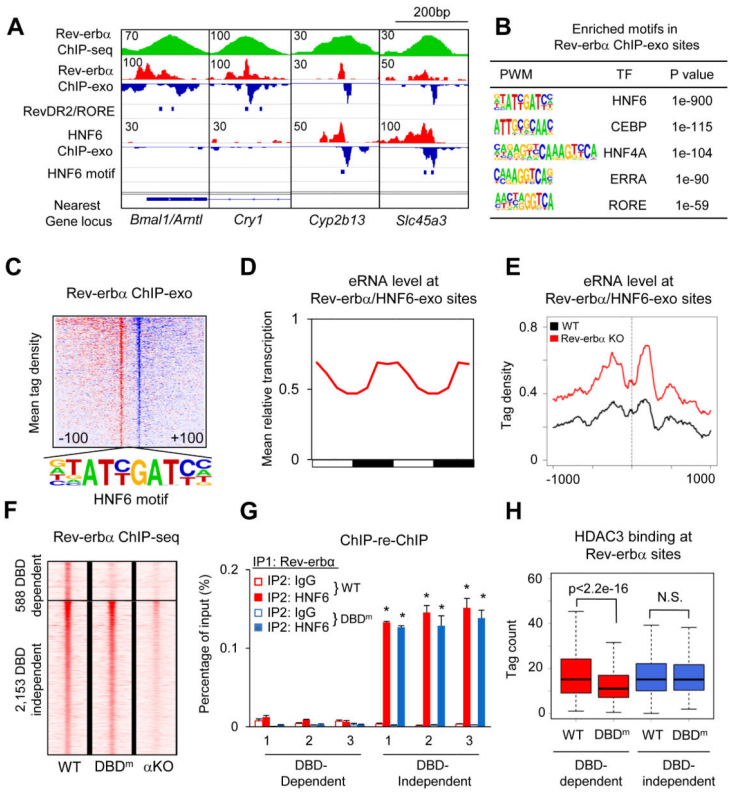

Figure 2. Rev-erbα binds to the genome using both DBD-dependent and DBD-independent mechanism

(A) Genome browser view of Rev-erbα and HNF6 ChIP-exo signals under Rev-erbα ChIP-seq peaks near clock and metabolic genes. Blue bars indicate locations of RevDR2/RORE and HNF6 motif. (B) Highly enriched known motifs found in Rev-erbα ChIP-exo peak pairs 22-26bp apart. (C) Heat map showing 5'-end tag densities of Rev-erbα ChIP-exo centered at HNF6 motifs within 1,108 peak pairs. Red and blue indicate tag density on the plus and minus strand, respectively. (D) Mean relative eRNA transcription (*22*) at Rev-erbα/HNF6-exo sites throughout 24-hour light dark cycles. Data were double plotted for clearer visualization. (E) eRNA tag density (*22*) centered at Rev-erbα/HNF6-exo sites near Rev-erbα target genes, in Rev-erbα KO and wild type liver. (F) Heat map showing Rev-erbα ChIP-seq tag densities (at ZT10) in wild type, DBD mutant (DBD^m), and Rev-erbα KO (αKO) mice, at DBD-dependent and -independent sites identified among 5,792 high confidence Rev-erbα peaks (peak height >1rpm, WT/Rev-erbα KO>3). (G) Sequential ChIP of Rev-erbα followed by either HNF6 or IgG ChIP in wild type and DBD^m mouse liver at ZT10. Data are expressed as mean± SEM (* Student's t-test, $p<0.05$, n=3 or 4 per group). (H) Binding of HDAC3 at DBD-dependent and -independent sites in WT and DBD^m liver (N.S. Student's t-test, $p>0.05$).

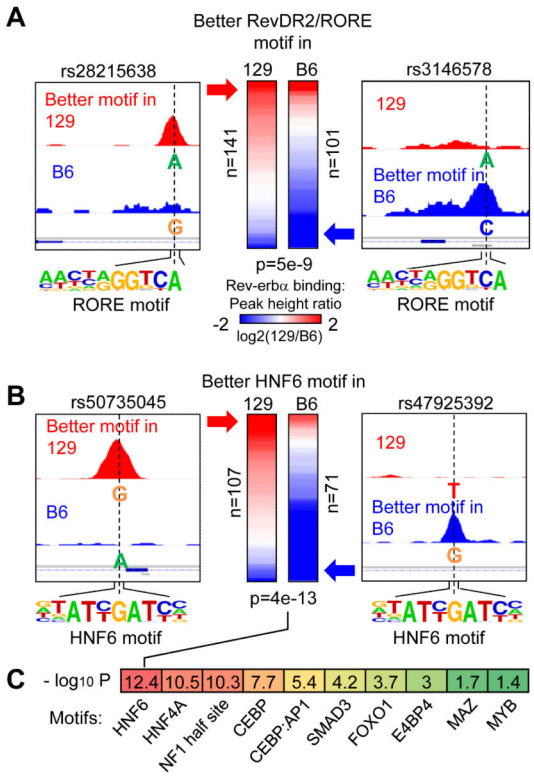

Figure 3. SNP associated strain-specific occupancy suggests HNF6-mediated binding of Rev-erbα

(A) Heat map showing $\log_2$ fold changes of Rev-erbα binding in 129 and B6 mice. The left column in the heat map contains 141 Rev-erbα peaks where RevDR2/RORE motif scores are higher in 129 mice and lower in B6 mice, due to the SNPs (illustrated in the left panel). Similarly, the right column contains 101 SNP-bearing Rev-erbα peaks with better RevDR2/RORE in the B6 genome. P value was calculated using Student's t-test. (B) Same analysis as in A, focusing on SNPs disrupting HNF6 motif under Rev-erbα peaks. (C) Heat map showing −log10 p values for other motifs that are enriched in DBD-independent Rev-erbα peaks.

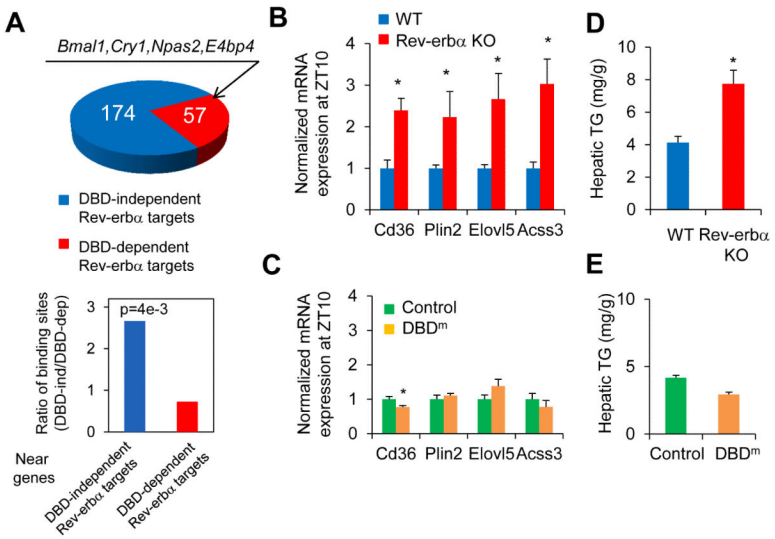

Figure 4. DBD-independent Rev-erbα sites regulate metabolic genes in liver

(A) Top panel shows the number of DBD-dependent and -independent Rev-erbα target genes identified using microarrays in Rev-erbα KO (*9*) and DBD^{m} mice (*12*). Bar graph shows ratios of DBD-independent and -dependent Rev-erbα/HDAC3 binding sites (*29*) located near two groups of Rev-erbα target genes (P value from hypergeometric test). (B) mRNA expression of lipid metabolic genes normalized to *Arpp*, measured by RT-qPCR, in livers of Rev-erba KO mice and wild type mice at ZT10. (C) mRNA expression of lipid metabolic genes normalized to *Arpp*, measured by RT-qPCR, in livers of Rev-erbα DBD^{m} (Rev-erbα/β double floxed mice injected with AAV-Tbg-Cre) or control mice (floxed mice injected with AAV-Tbg-GFP) at ZT10. Data are expressed as mean± SEM (* Student's t-test, $p<0.05$, n=4 per group). (D) Hepatic triglyceride (TG) levels in the same mice as in B. (E) Hepatic TG levels in mice as in C (* Student's t-test, $p<0.05$, n=4 per group).